High-Energy X-ray Compton Scattering for Non-destructive and Quantum Characterization in Batteries

***Kosuke Suzuki[1], H. Sakurai[1], N. Tsuji[2], Y. Sakurai[2], Y. Orikasa[3], Y. Uchimoto[4], H. Hafiz[5,6], B. Barbiellini[7,6] and A. Bansil[6]**

* kosuzuki@gunma-u.ac.jp

[1]*Faculty of Science and Engineering, Gunma University*
[2]*Japan Synchrotron Radiation Research Institute (JASRI), SPring-8*
[3] *Department of Applied Chemistry, Ritsumeikan University*
[4]*Graduate School of Human and Environmental Studies, Kyoto University*
[5]*Department of Mechanical Engineering, Carnegie Mellon University*
[6]*Department of Physics, Northeastern University*
[7]*School of Engineering Science, Lappeenranta University*

Contents

Introduction

Although lithium-ion batteries are already widely used in our daily life, further development of high-performance batteries are expected.

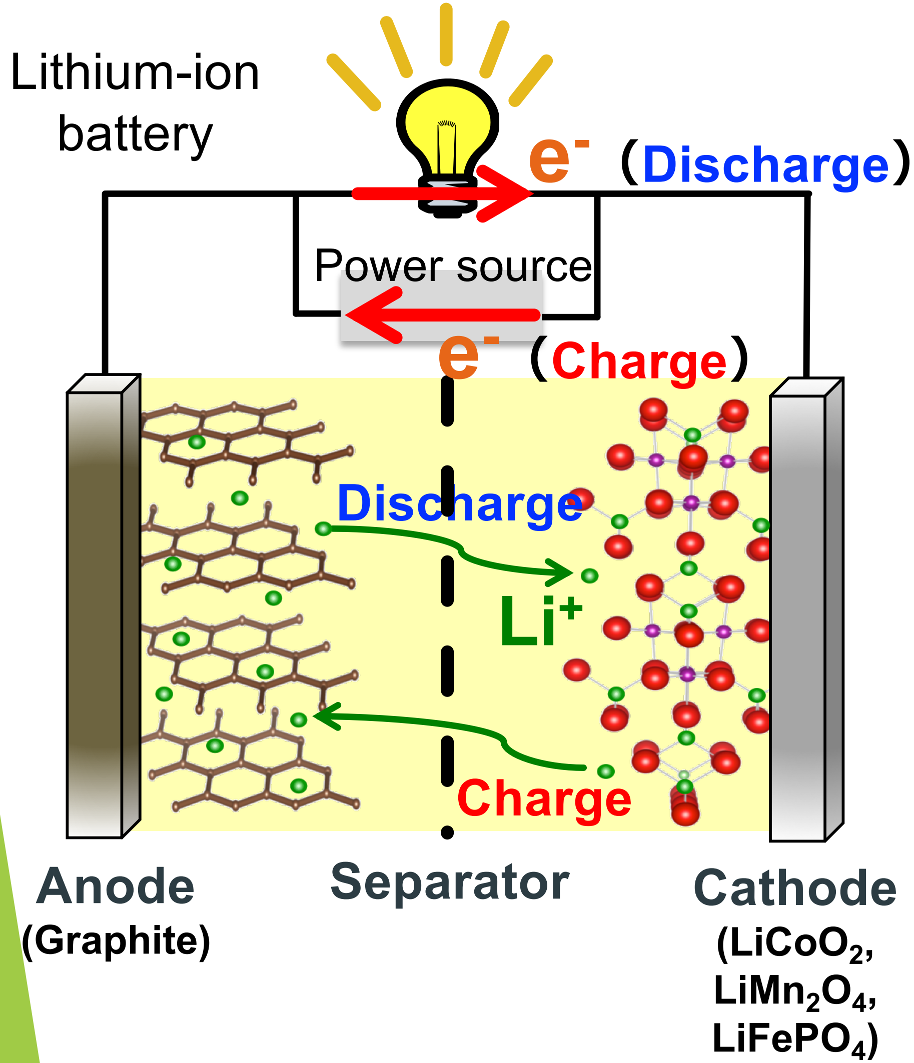

➢ Problems in real battery

- **Inhomogeneous lithium reaction**
- **Capacity degradation**

Non-destructive measurement

➢ Problems in material

- **High-capacity electrode materials**
- **High-stability electrode materials**

Understanding of electrode reaction

We focus on Compton scattering technique to resolve these problems.

Compton scattering

Compton scattering is well known as inelastic scattering technique between photons and electrons.

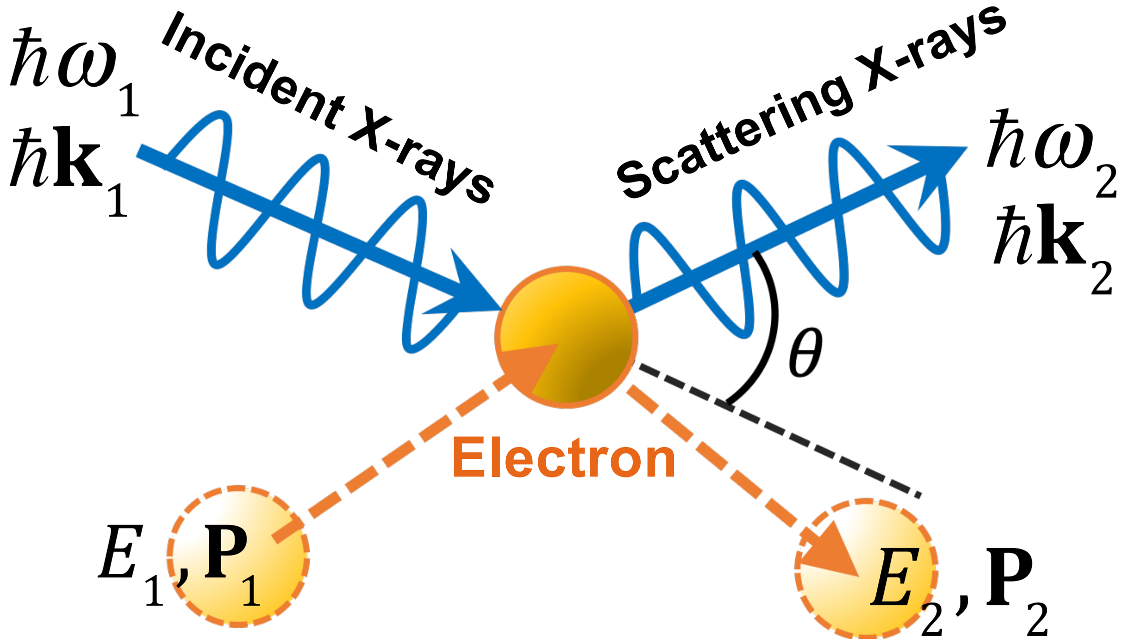

- **Energy conservation law**

$$\hbar\omega_1 + E_1 = \hbar\omega_2 + E_2$$

- **Momentum conservation law**

$$\hbar\mathbf{k}_1 + \mathbf{p}_1 = \hbar\mathbf{k}_2 + \mathbf{p}_2$$

- **Scattered X-ray energy**

$$\hbar\omega_2 = \hbar\omega_1 - \frac{\hbar^2|\mathbf{k}|}{2m} - \frac{\hbar\mathbf{k}\cdot\mathbf{p}_1}{m}$$

$\hbar\omega_1, \hbar\omega_2$: Photon energy

$\hbar\mathbf{k}_1, \hbar\mathbf{k}_2$: Photon momentum

E_1, E_2 : Electron energy

$\mathbf{p}_1, \mathbf{p}_2$: Electron momentum

Compton profile

- Scattered X-ray energy

$$\hbar\omega_2 = \hbar\omega_1 - \frac{\hbar^2|\mathbf{k}|}{2m} - \frac{\hbar\mathbf{k}\cdot\mathbf{p}_1}{m}$$

- **Energy spectrum :** $I(\hbar\omega_2)$

$$I(\hbar\omega_2) \propto J(p_z)$$

- **Compton profile :** $J(p_z)$

$$J(p_z) = \iint \rho(\mathbf{p})\, dp_x\, dp_y$$

- **Electron momentum density :** $\rho(\mathbf{p})$

$$\rho(\mathbf{p}) = \sum_j n_j \left| \int \psi_j(\mathbf{r}) \exp(-i\mathbf{p}\cdot\mathbf{r})\, d\mathbf{r} \right|^2$$

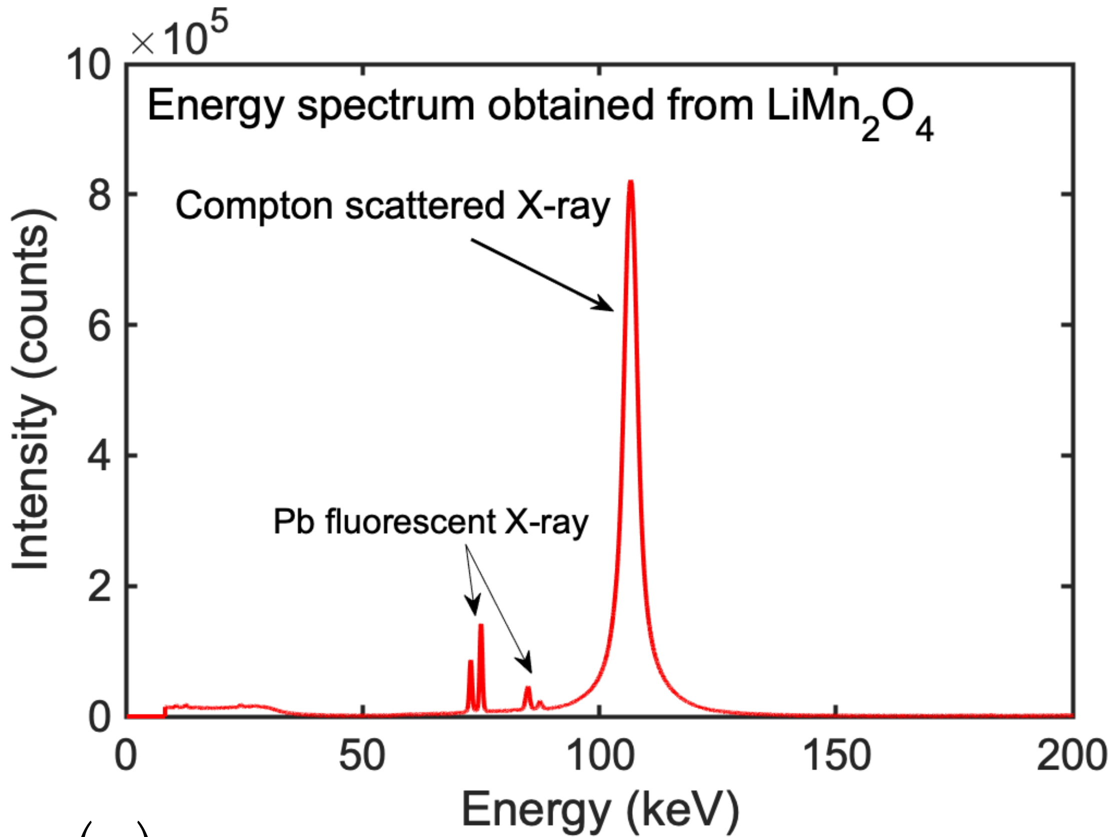

$\hbar\omega_2$: Scattered X-ray energy
$\mathbf{p} = (p_x, p_y, p_z)$: Electron momentum
n_j : Occupation number
$\psi_j(\mathbf{r})$: *j*-th wavefunction

Compton profile can directly compare with theoretical Compton profile.

It is enables to discuss electronic structure underlying reduction-oxidation reaction on the electrodes.

Advantage of Compton scattering

Compton scattering technique have mainly two advantages.

(1) High-energy (>100keV) X-rays

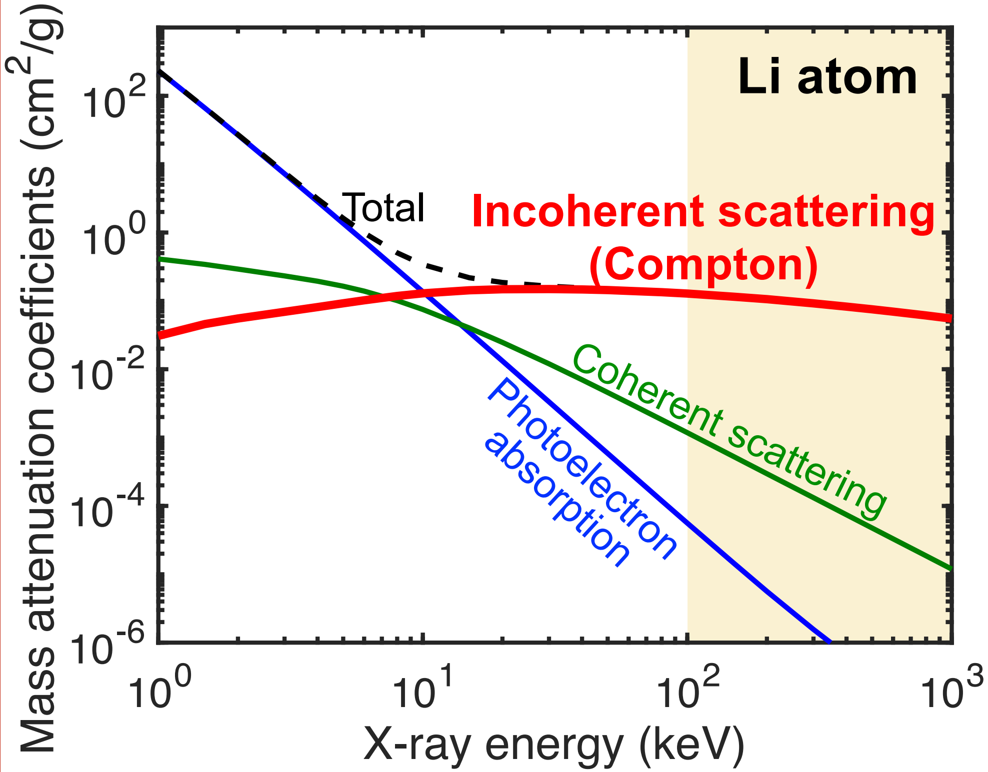

Incoherent scattering is enhanced by using over 100keV X-rays.

NIST (http://www.nist.gov)

(2) Line-shape of Compton profile

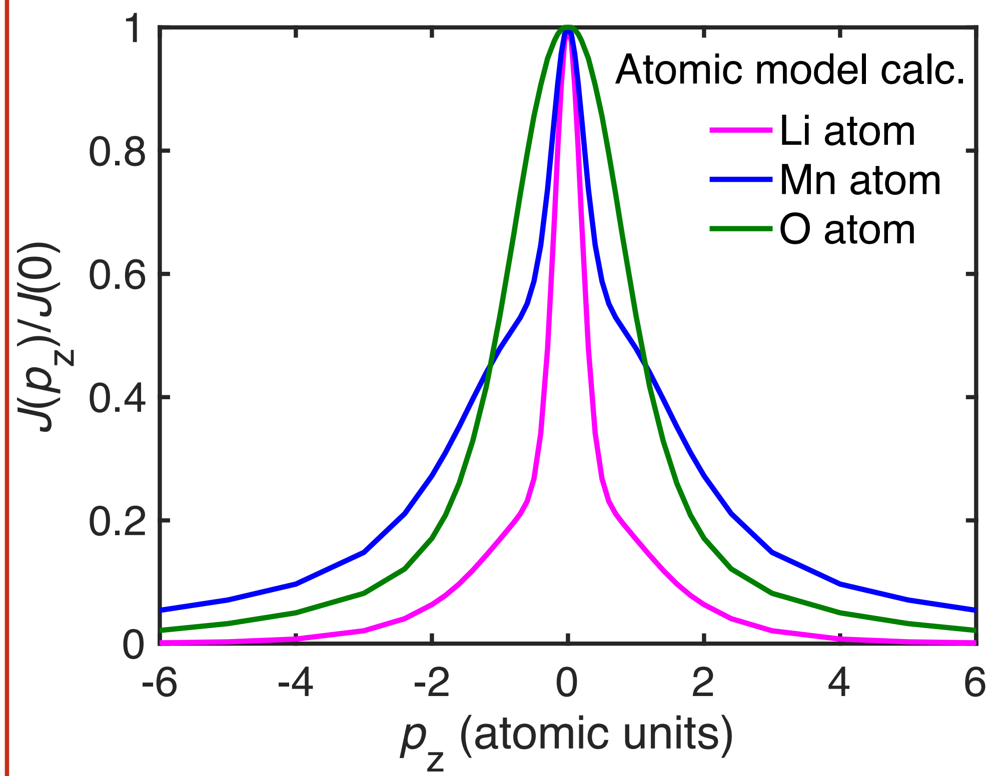

Quantitative analysis will be possible by digitalizing the line-shape of Compton profile

Biggs et al., Atomic Data and Nuclear Data Tables 16, 201 (1975).

These features are suitable for analyzing lithium-ion batteries.

Shape-parameter (*S*-parameter)

We have developed analysis method using a shape-parameter (*S*-parameter) to analyze line-shape of Compton profile.

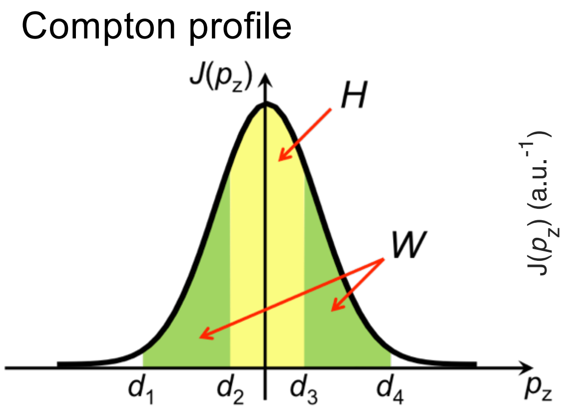

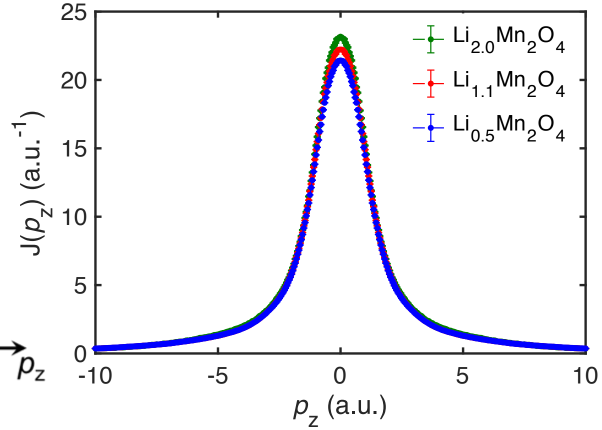

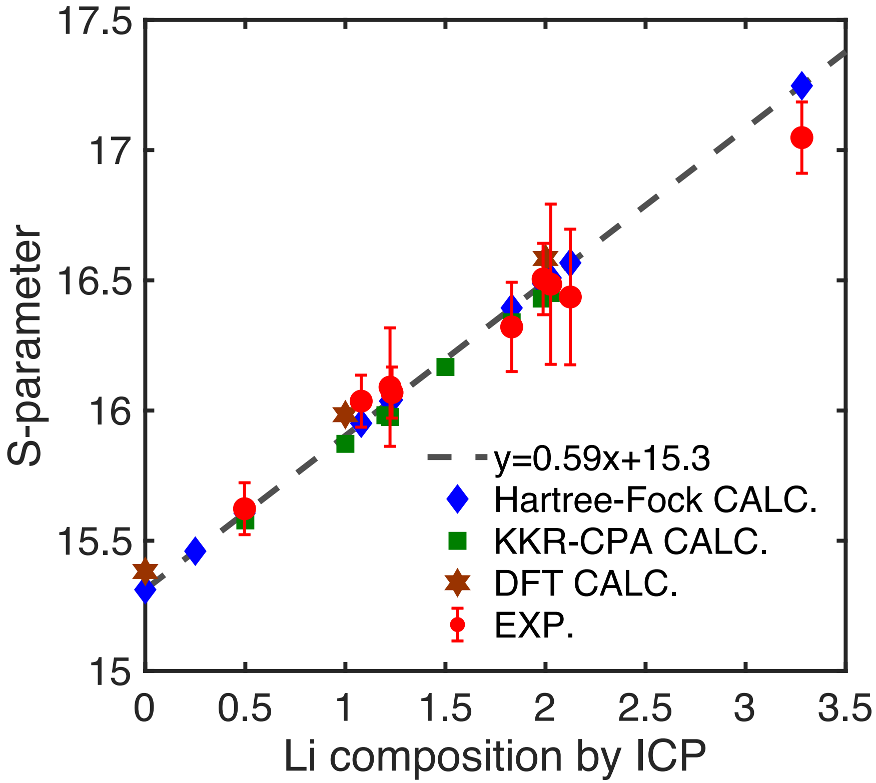

$$S = \frac{H}{W}$$

$$H = \int_{d_2}^{d_3} J(p_z)\, p_z$$

$$W = \int_{d_1}^{d_2} J(p_z)\, p_z + \int_{d_3}^{d_4} J(p_z)\, p_z$$

In this study, d_1=d_4=5a.u., d_2=d_3=1a.u. were decided.

Linear relationship between *S*-parameters and lithium concentration is confirmed.

Lithium quantitation is possible by using *S*-parameter analysis.

K. Suzuki et al., J. Appl. Phys., 119, 025103 (2016).

Non-destructive characterization for real batteries

Compton scattering technique is applied to commercial VL2020 coin battery to observe lithiation state

Non-destructive measurement

Many experimental techniques are demonstrated to monitor lithium reactions.

- **X-ray absorption near-edge structure (XANES)** ・・・ **Test cell**
  C. Rumble et al., J. Electrochem. Soc., 157, A1317 (2010).
  H. Arai et al., J. Mater. Chem., 1, 10442 (2013).
  M. Katayama et al., J. Power Sources, 269, 994 (2014).
- **Nuclear magnetic resonance (NMR)** ・・・ **Test cell**
  S. Chandrashekar et al., Nature Mat., 11, 311 (2012).
- **Micro X-ray diffraction** ・・・ **Test cell**
  J. Liu et al., J. Phys. Chem. Lett., 1, 2120 (2010).
- **Particle induced γ–ray/X-ray emission (RIGE/PIXE)** ・・・ **Test cell**
  K. Mima et al., Nucl. Instrum. Methods Phys. Rev. B 290, 79 (2012).
- **Raman micro-spectroscopy** ・・・ **Test cell**
  T. Nishi et al., J. Electrochem. Soc., 160, A1785 (2013).
- **Hard X-ray photoemission spectroscopy (HX-PES)** ・・・ **Cylindrical cell**
  H. Hori et al., J. Power Sources, 242, 844 (2013).
- **Neutron diffraction** ・・・ **Cylindrical cell**
  Xun-Li Wang et al., Scientific Reports, 2, 1 (2012).

These experiments are mainly adopted to the test cells and It is difficult to measure Li directly.

We focus on Compton scattering technique.

Sample and Experimental setup

➢ **Sample (Panasonic VL2020)**

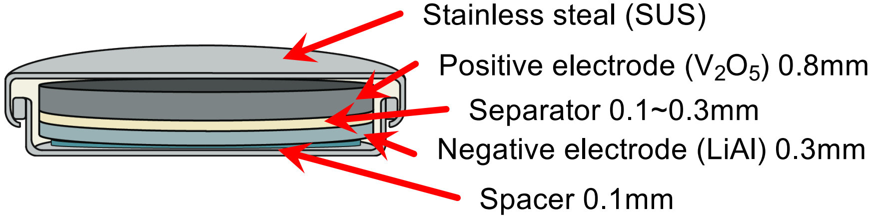

➢ **Experiment setup (BL08W SPring-8)**

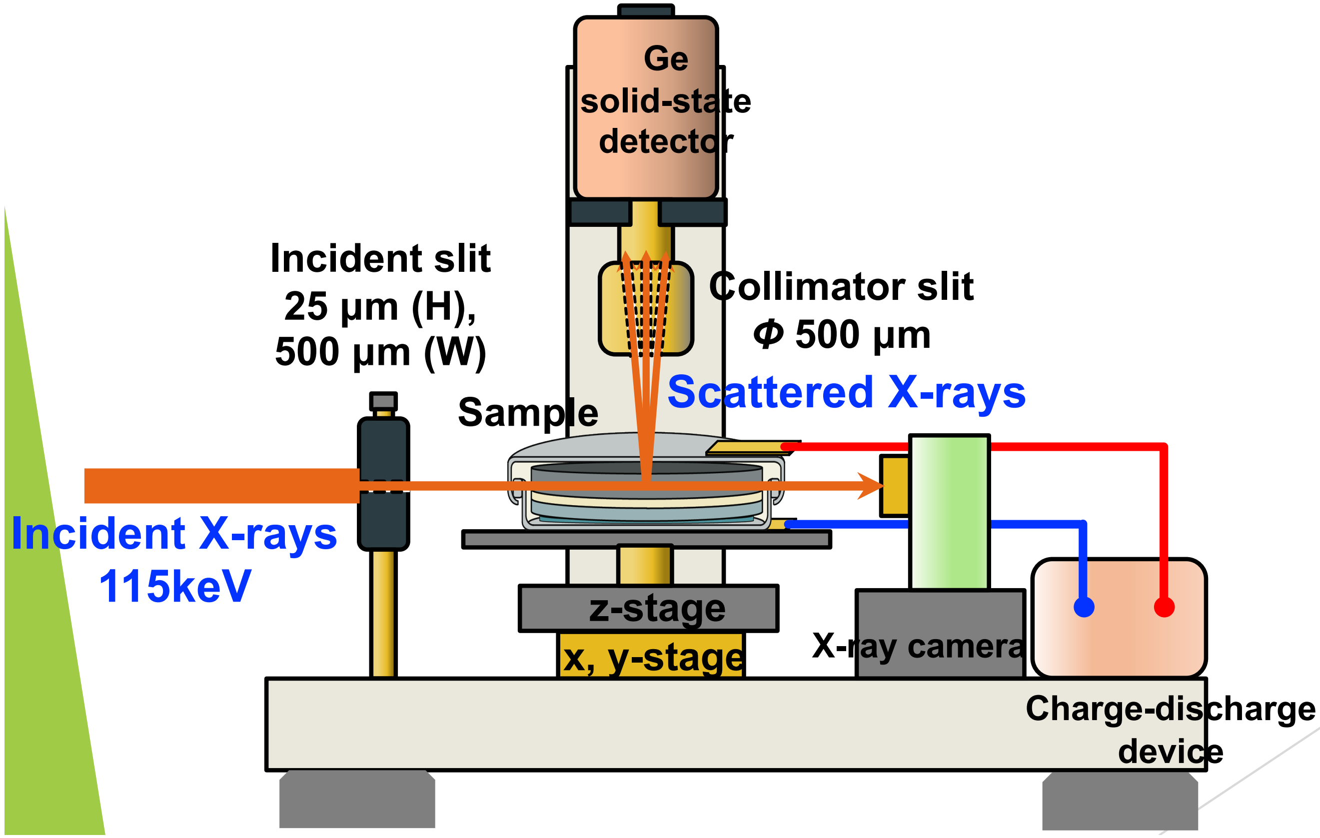

SPring-8 BL08W

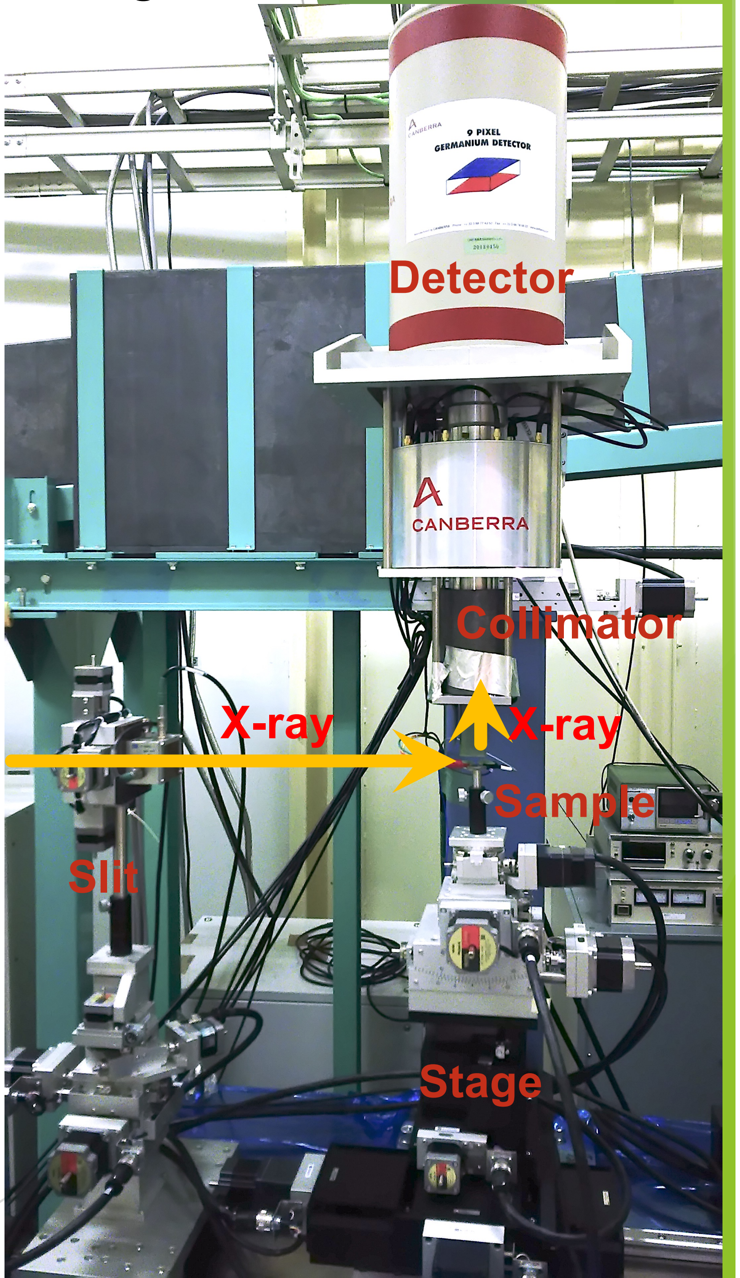

Energy spectrum and *S*-parameter

Energy spectrum was measured in order to distinguish battery components.

Energy spectra

Energy spectrum of SUS, electrodes and separator was measured.

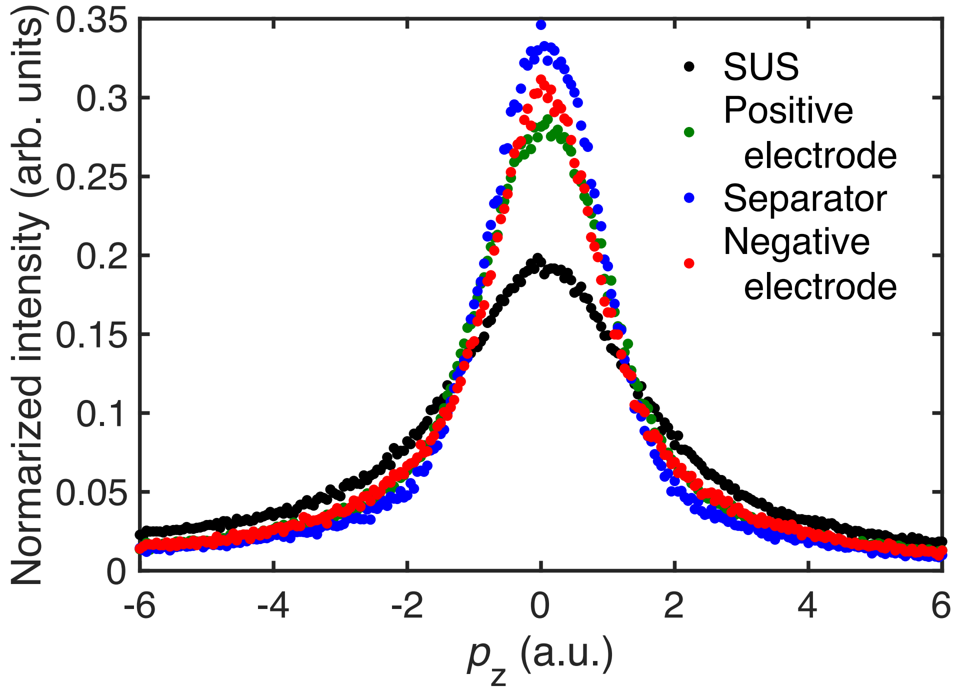

Energy spectra change with the components of the battery.

S-parameter

Energy spectrum was converted to *S*-parameter.

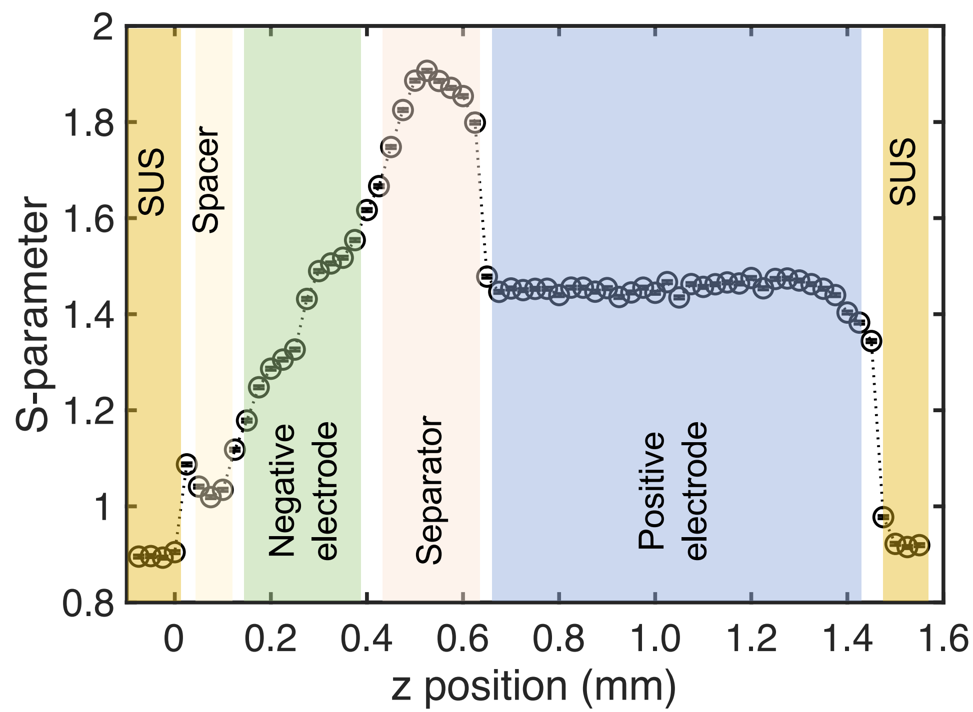

***S*-parameters can reveal internal structure of the battery.**

K. Suzuki et al., J. Synchrotron. Rad., 24, 1006 (2017).

S-parameter distribution

S-parameter distribution during charge-discharge cycle was obtained.

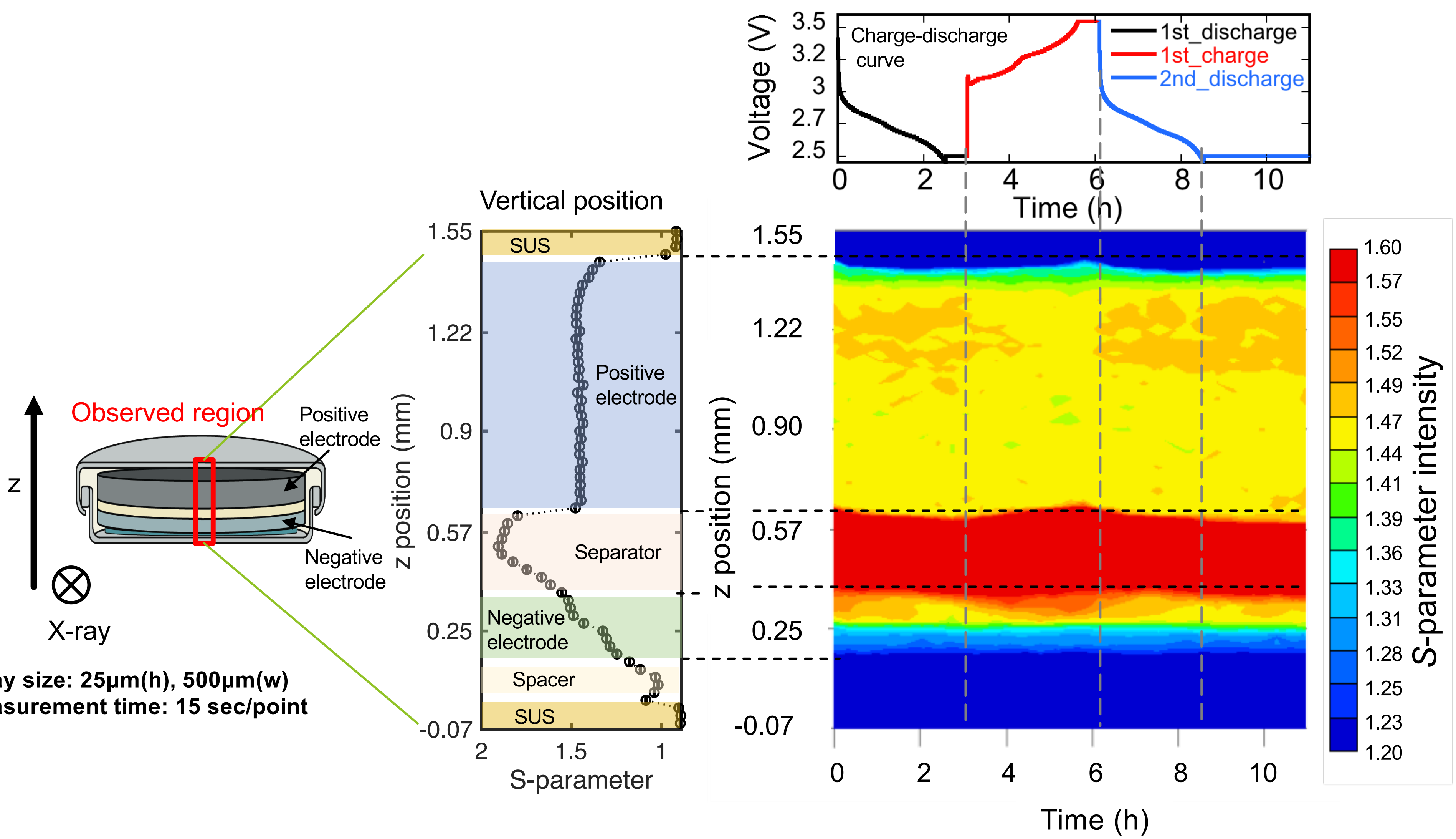

X-ray size: 25μm(h), 500μm(w)
Measurement time: 15 sec/point

K. Suzuki et al., J. Synchrotron. Rad., 24, 1006 (2017).

ΔS-parameter distribution

In order to clarify the change of S-parameter at the positive and negative electrodes, ΔS-parameter is taken.

$\Delta S = S_t - S_{ave}$

S_t: S-parameter at t sec
S_{ave}: averaged S-parameter on total measurement time

When the battery charged, high *S*-parameter region exist in the separator.

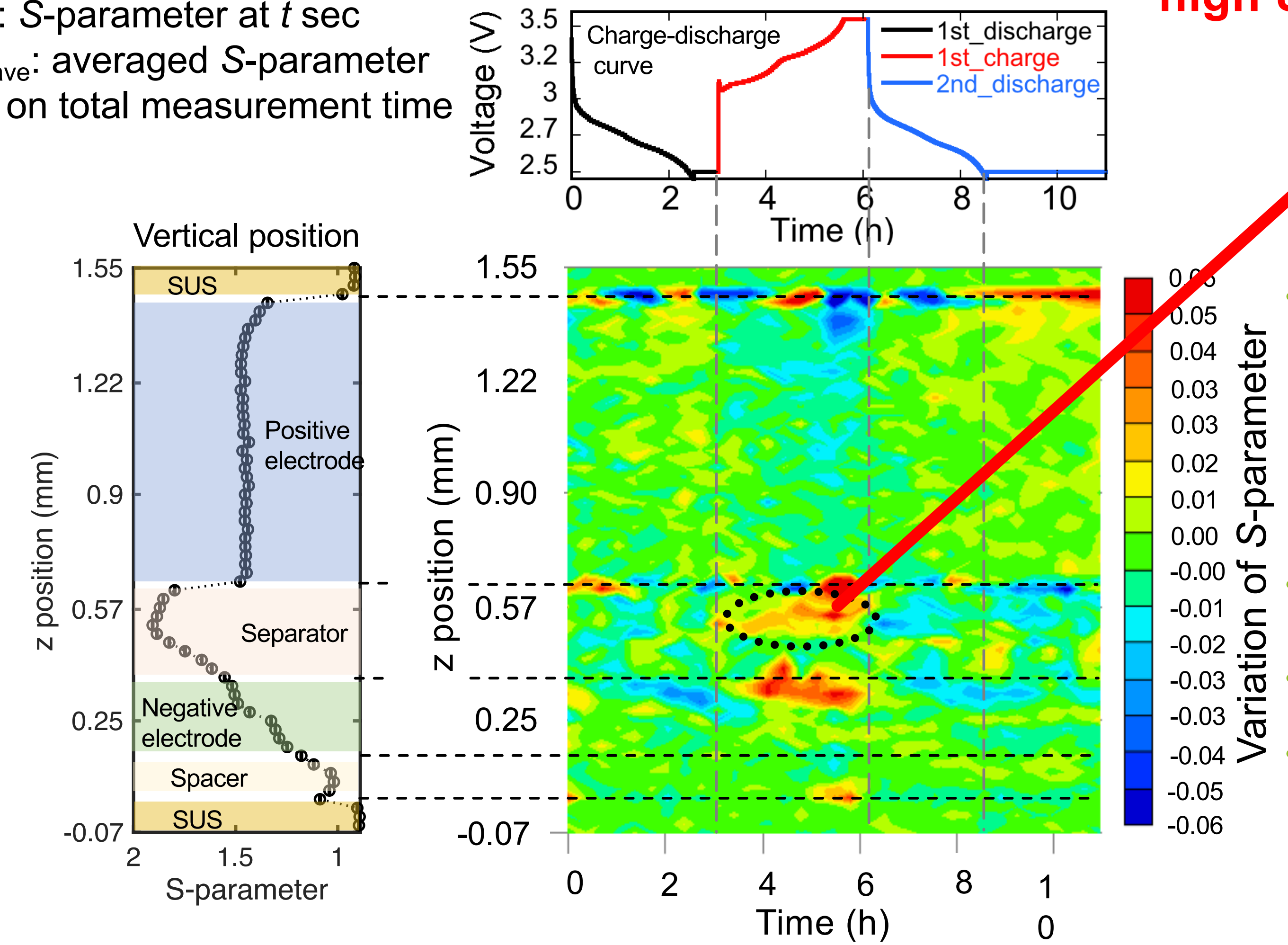

Positive electrode

Uniform reactions are occurred.

Negative electrode

The reactions occur at the surface.

K. Suzuki et al., J. Synchrotron. Rad., 24, 1006 (2017).

S-parameter at the separator

Raw data of *S*-parameters around the separator position.

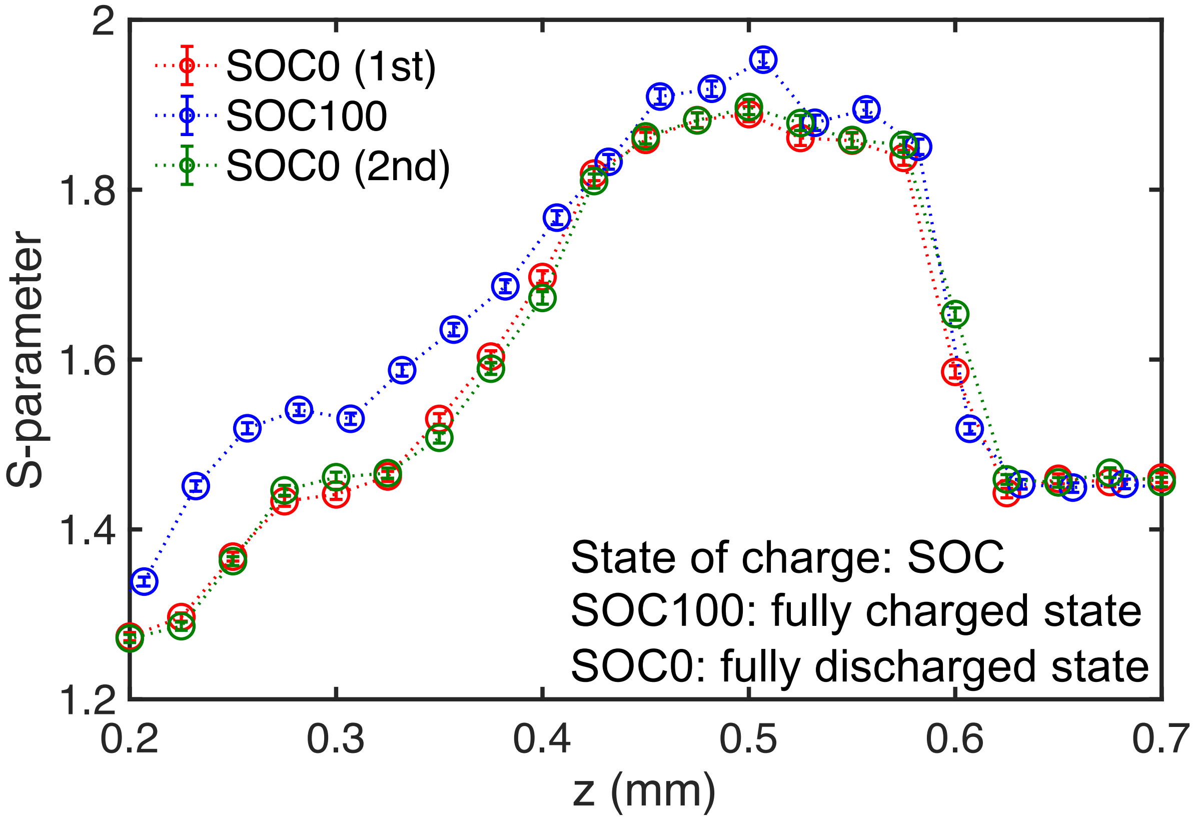

- The reproducibility was confirmed between 1st and 2nd full discharged state.
- The *S*-parameters increase at the separator position when full charged state.

Some lithium-ions remain into the separator.
This fact might be induce capacity loss of the battery.

Lithium composition

Lithium compositions during charge-discharge cycle are determined.

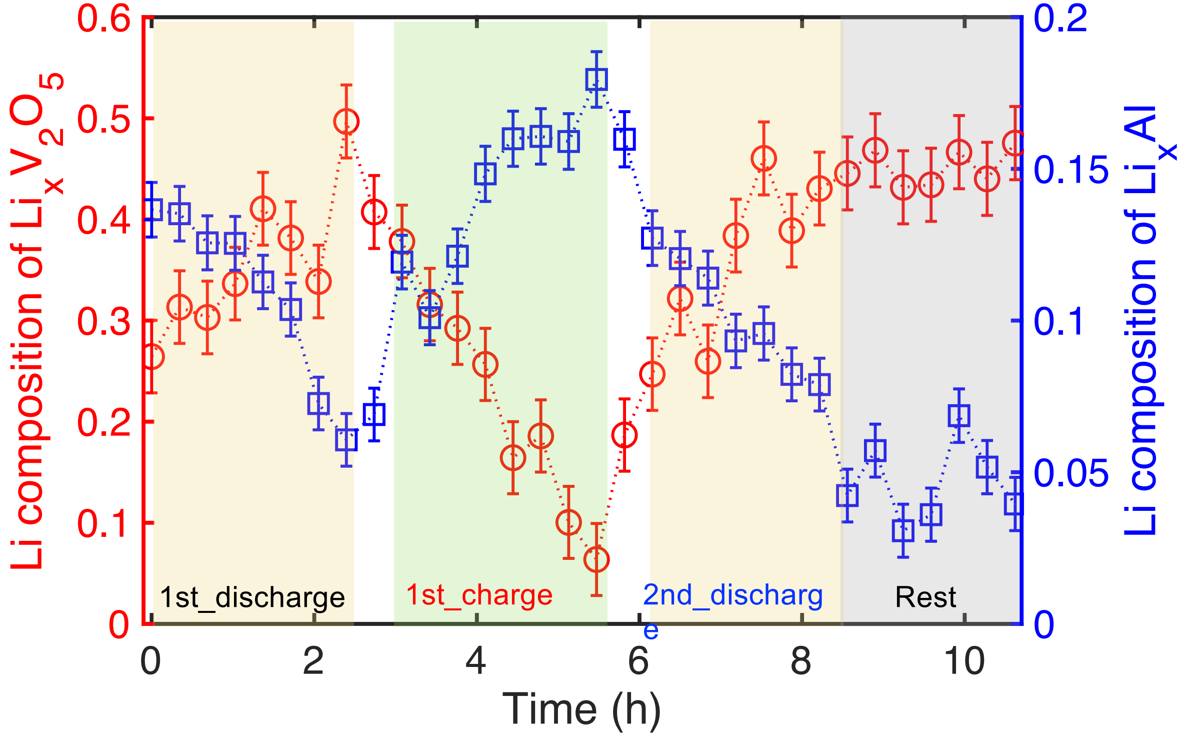

Li composition	ICP analysis	*S*-parameter
Positive electrode SOC0	0.426	**0.470±0.012**
Negative electrode SOC100	0.178	**0.170±0.006**

Li composition is agree with that of obtained from ICP analysis.

Non-destructive and in-operando analysis are possible by our technique.

Quantum characterization for battery materials

High-resolution Compton scattering and magnetic Compton scattering experiments are applied to $LiMn_2O_4$ to reveal electrode reaction

$LiMn_2O_4$

Spinel $LiMn_2O_4$ is a representative positive electrode material for lithium-ion batteries.

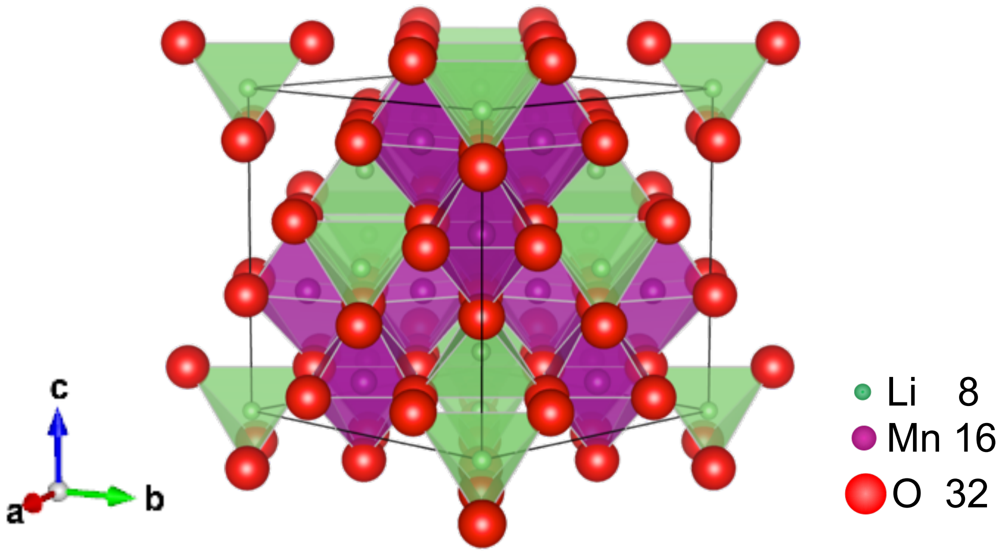

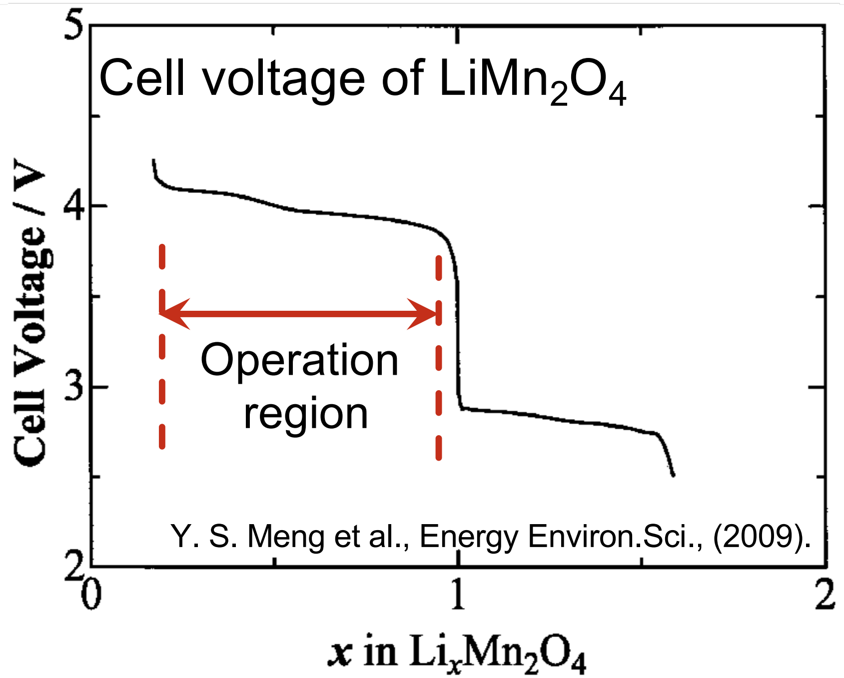

Advantage

- **Thermodynamic stability**
- **Low cost**

Disadvantage

Charge/discharge curve

L. Guohua et al., J. Electrochem. Soc., 143 (1996) 178

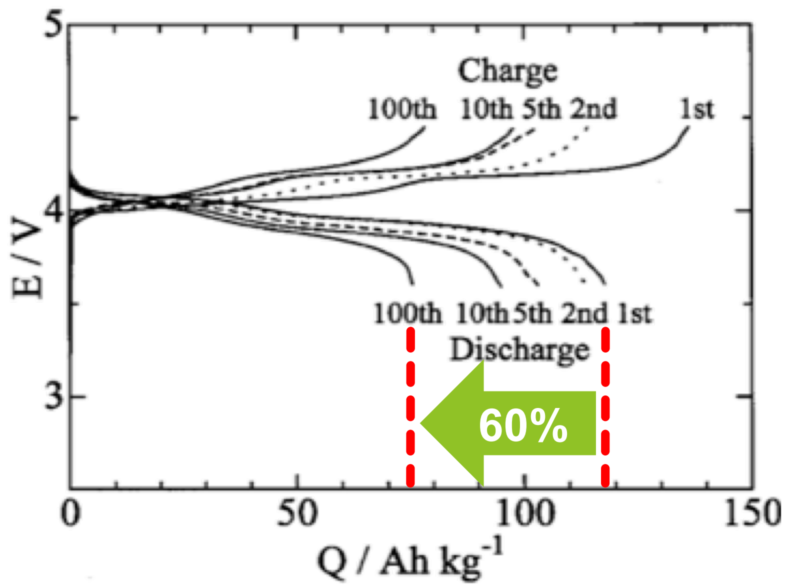

The capacity decreases 60% at 100 cycles

Electrode reaction of $LiMn_2O_4$

$LiMn_2O_4$ (+3.5) — Charge → / ← Discharge — $xLi^+ + Li_{(1-x)}Mn_2O_4 + xe^-$ (+4)

The volume expansion by Jahn-Teller ion induces capacity loss

- ♦ LMTO-ASA（H. Berg et al., J. Mater. Chem.9, 2813 (1999))
- ♦ FP-LMTO（G. E. Grechnev et al., Phys. Rev. B65, 174408 (2002)）

On the other hand

- ♦ DV-Xα（Y. Liu et al., Solid State Ionics,126, 209 (1999)）
- ♦ LDDFT（M. K. Aydinol et al., J. Electrochem., 144, 3832 (1997)）

O 2*p* orbital plays important role

The electrode reaction is not fully understood yet.

The nature of the electrode reaction is investigated.

Previous study

Compton profiles of $Li_xMn_2O_4$ (x = 0.496 and 1.079) were measured.

The difference Compton profile are shown with KKR-CPA first-principle calculation result.

Sample

$Li_xMn_2O_4$ powder

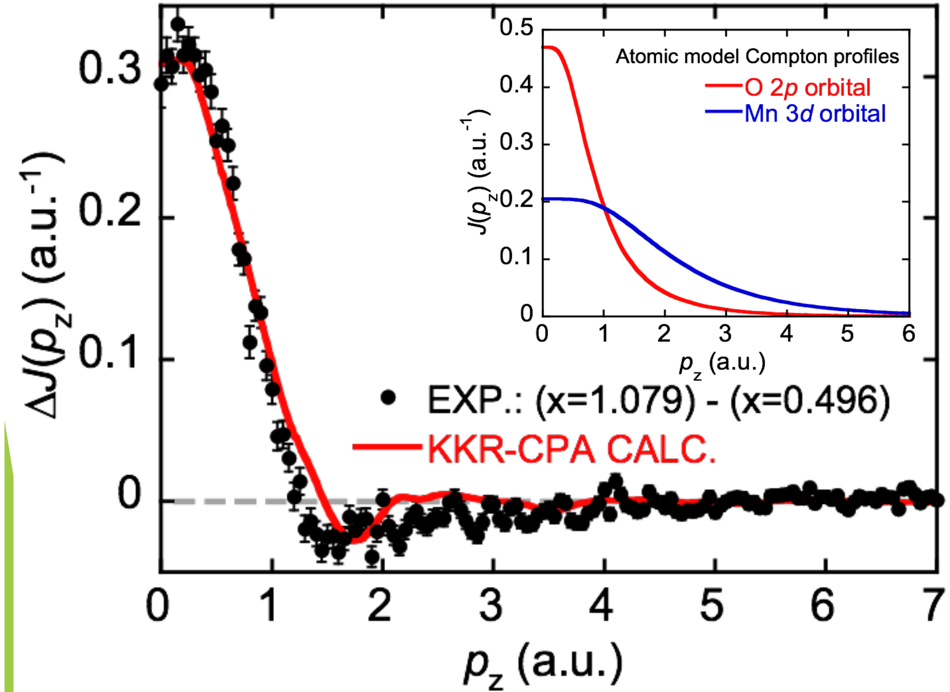

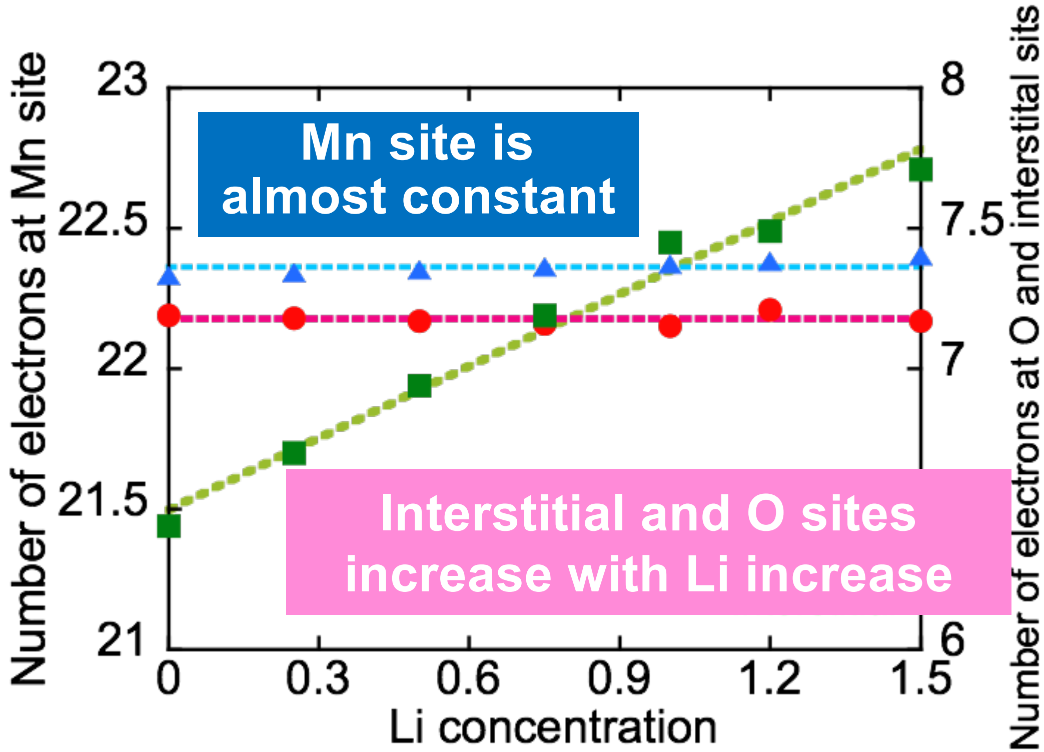

The O 2p orbitals play a dominant role on the electrode reaction of $LiMn_2O_4$ positive electrode.

Magnetic Compton scattering is applied to study electronic structure of Mn atom.

K. Suzuki et al., PRL, 114, 087401 (2015).

Magnetic Compton profile (MCP)

Magnetic Compton profiles of $Li_xMn_2O_4$ (x = 0.41, 0.50 and 0.92) were measured.

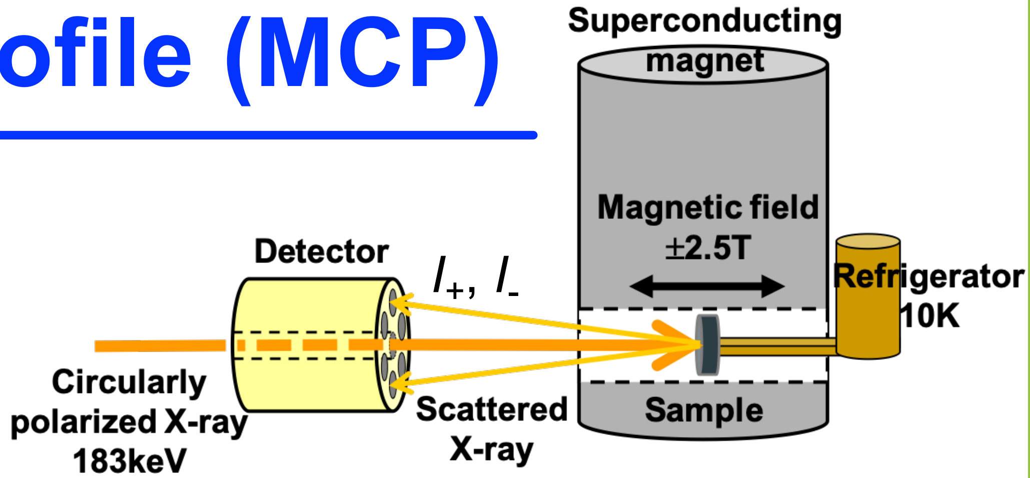

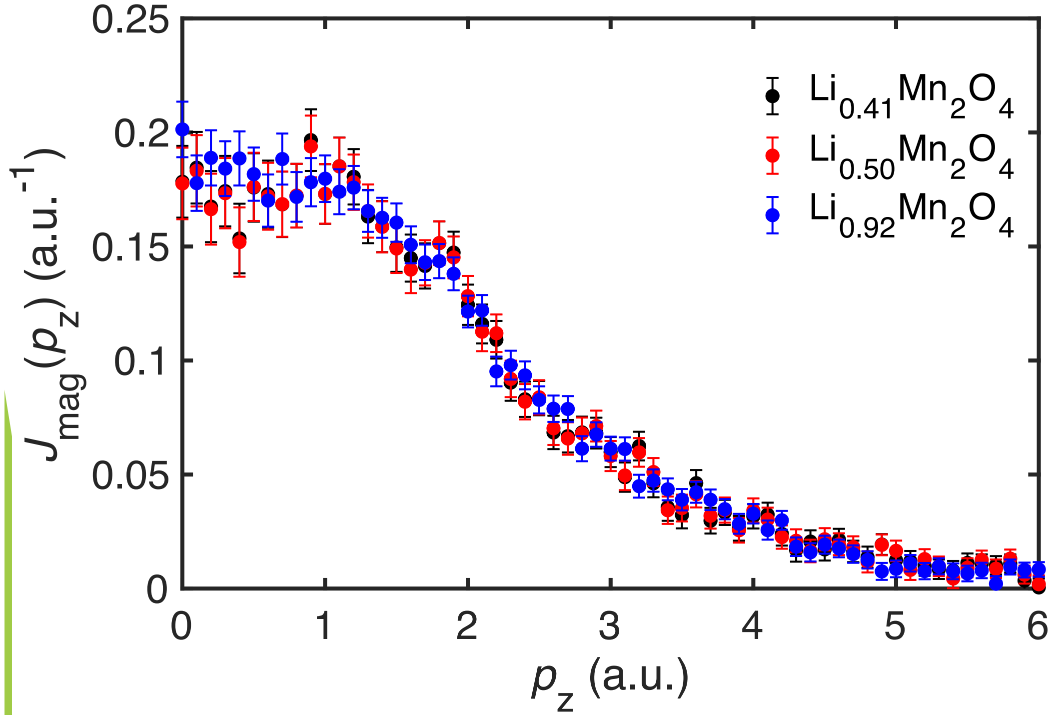

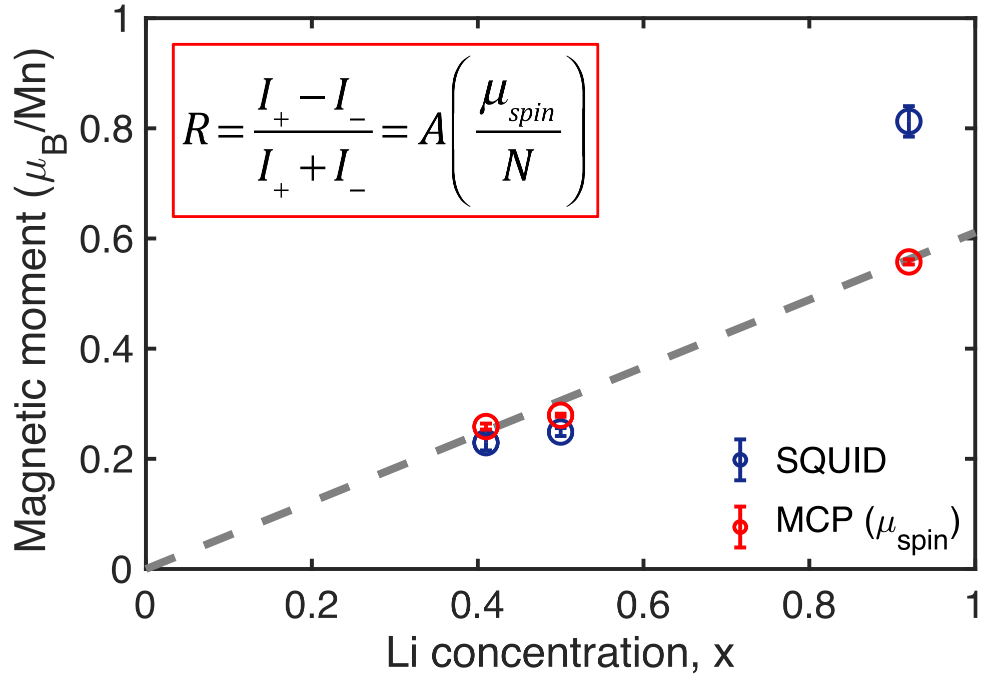

The line-shape of MCPs does not show significantly change.

Spin magnetic moment increase with increasing Li concentration.

We do comparison with theoretical calculation results to reveal increase of spin magnetic moments in operation region of the battery.

Theoretical MCP and magnetic moment

Theoretical magnetic Compton profile was calculated by first-principle DFT calculation using exchange-correlation function of SCAN meta-GGA.

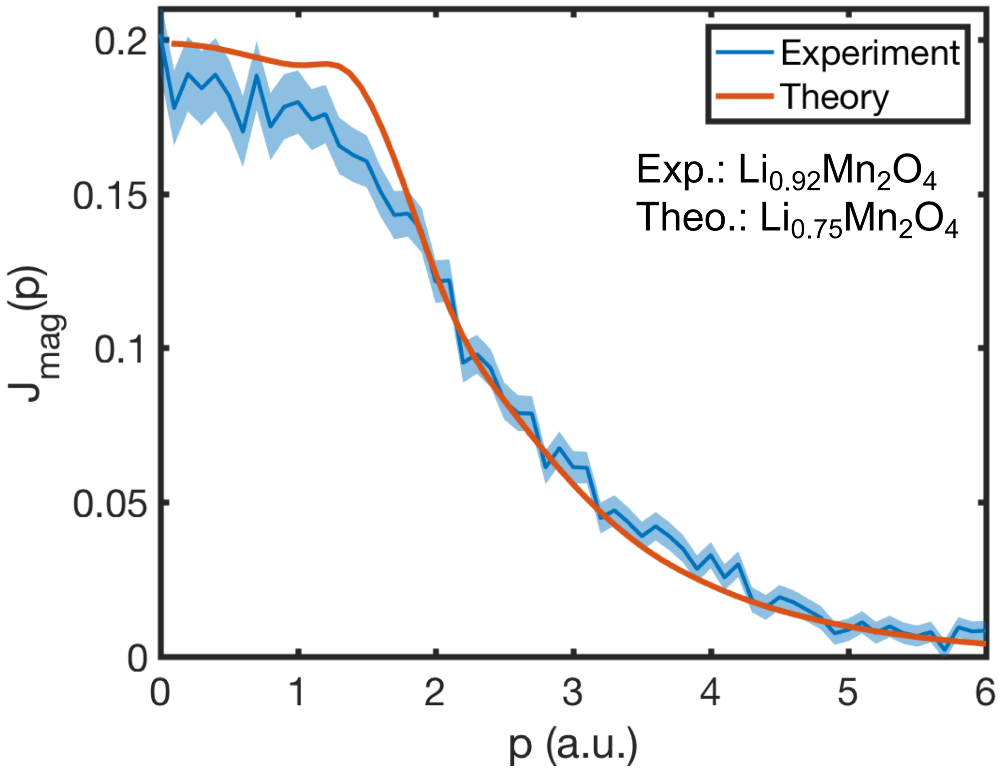

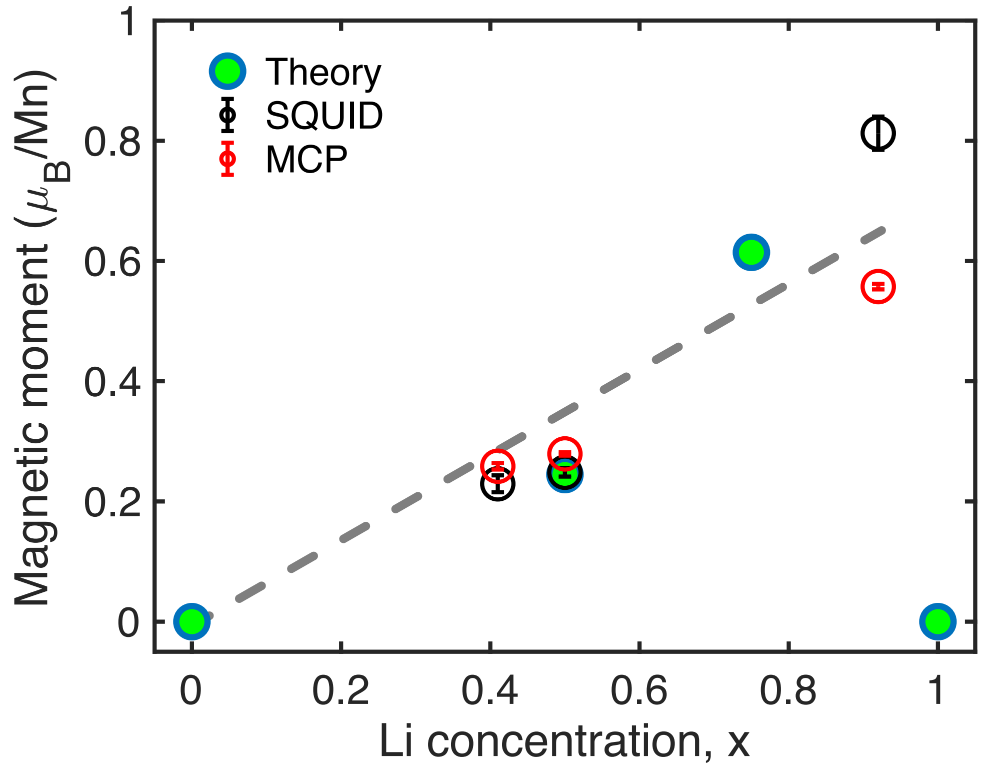

Calculated spin magnetic moment in lithium concentration 0 < x <1 have same trend with experimental spin magnetic moment.

H. Hafiz et al., PRB, submitted.

Spin-dependent partial density of state

Spin-dependent partial density of state associated with the e_g and t_{2g} orbitals of Mn^{3+} and Mn^{4+} ions are calculated.

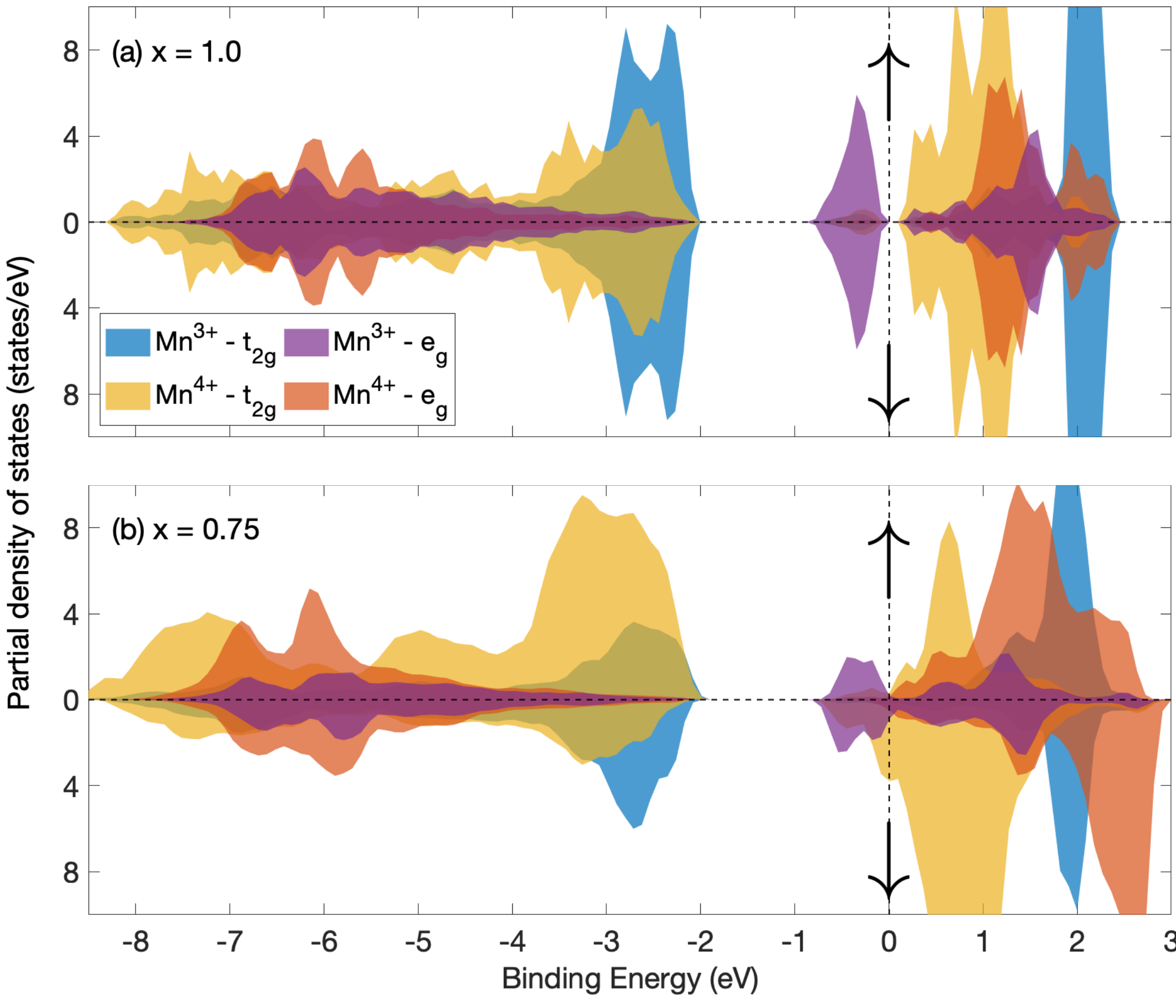

The Mn e_g orbital split and Mn $3d_{z^2}$ bands move to lower energies

$LiMn_2O_4$ has band gap

Mn $3d_{z^2}$ bands are partially occupied

$Li_{0.75}Mn_2O_4$ becomes metallic and have ferrimagnetic state

H. Hafiz et al., PRB, submitted.

Magnetic structure

Magnetic configuration models are considered.

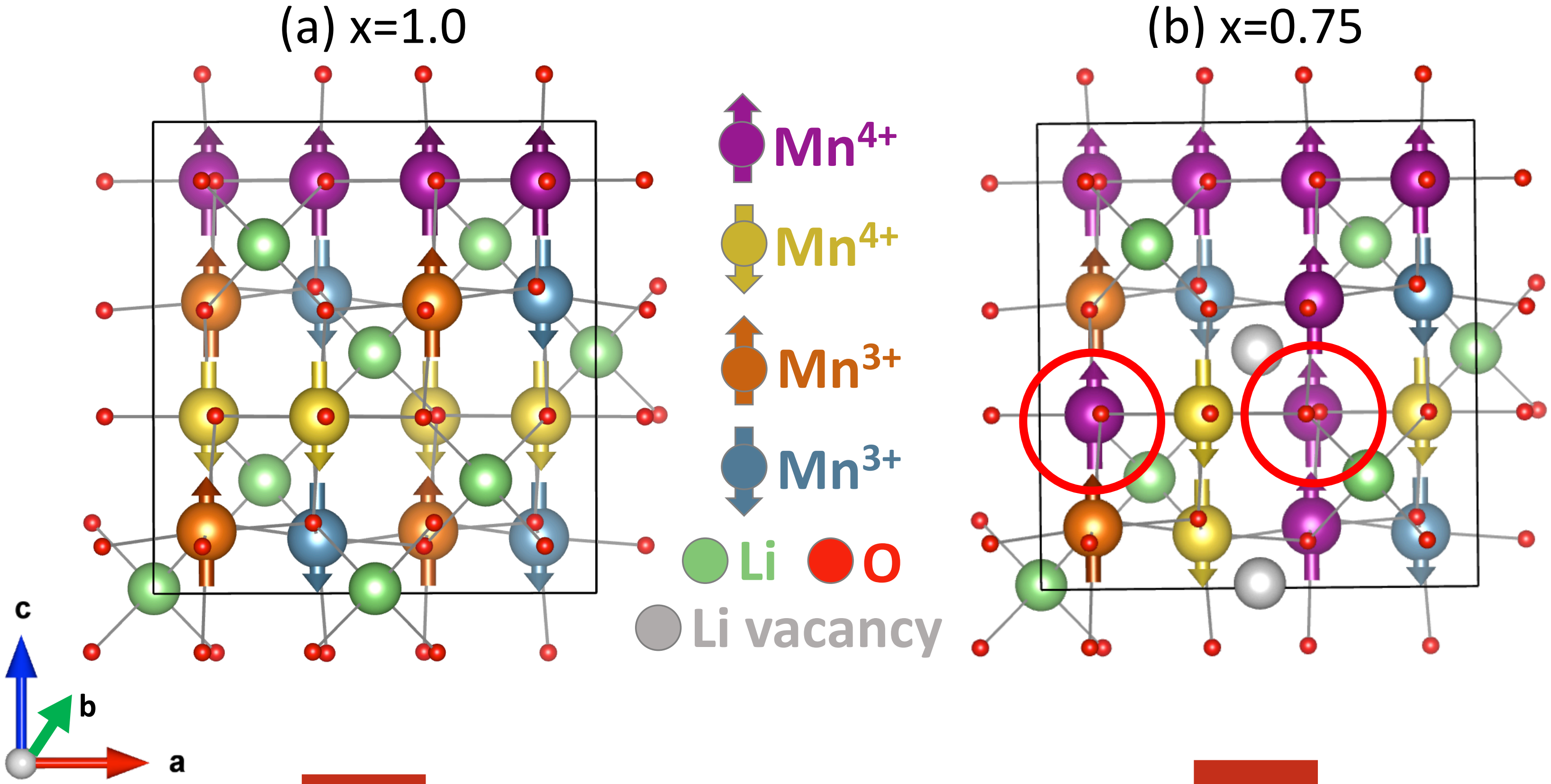

Charge-ordering is prominent.

Charge-ordering become unstable, and spin-flipping of Mn^{4+} is occur.

H. Hafiz et al., PRB, submitted.

Magnetic orbital

Magnetic orbital of $Li_{0.75}Mn_2O_4$ is visualized.

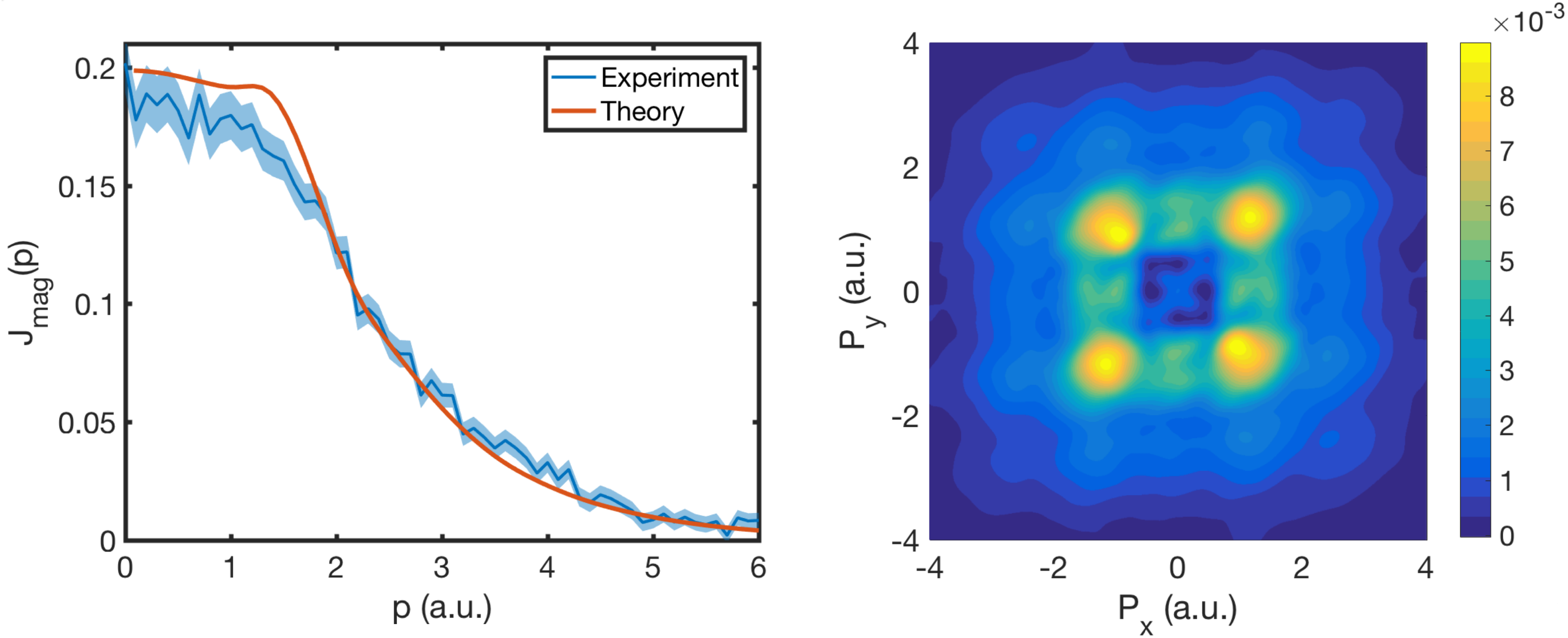

Mn 3d magnetic electrons in $Li_xMn_2O_4$ (x < 1) have mainly t_{2g} symmetry, and they prevent structural distortion promoted by e_g character.

The O 2*p* orbitals play a dominant role on the electrode reaction and Mn 3d orbitals contribute to the stability of the structure in $LiMn_2O_4$.

Summary

Non-destructive characterization study for the commercial battery and quantum characterization study for the electrode material were shown.

- **Non-destructive characterization for VL2020 battery**
  - **Lithium reactions of the electrodes are revealed nondestructively.**
  - **Remnant lithium ions are observed in the separator when the battery was charged.**

- **Quantum characterization for $LiMn_2O_4$**
  - **The O 2*p* orbitals play a dominant role on the electrode reaction.**
  - **The Mn 3d orbitals contribute to the stability of the structure.**

Compton scattering technique is powerful tool for non-destructive and quantum characterizations in the batteries.